Structure, Magnetic Properties and ^{151}Eu, ^{119}Sn Mössbauer Spectroscopy of $Eu_5Sn_3S_{12}$ and $Eu_4LuSn_3S_{12}$

Petra Jakubcová[a], Dirk Johrendt[a], C. Peter Sebastian[b], Sudhindra Rayaprol[b], and Rainer Pöttgen[b]

[a] Department Chemie und Biochemie, Ludwig-Maximilians-Universität München, Butenandtstraße 5 – 13 (Haus D), D–81377 München, Germany
[b] Institut für Anorganische und Analytische Chemie and NRW Graduate School of Chemistry, Westfälische Wilhelms-Universität Münster, Corrensstraße 30, 48149 Münster, Germany

Reprint requests to Prof. Dr. D. Johrendt. E-mail: johrendt@lmu.de

Z. Naturforsch. **2007**, *62b*, 5 – 14; received August 21, 2006

$Eu_5Sn_3S_{12}$ and $Eu_4LuSn_3S_{12}$ were synthesized and their structures refined from single crystal data (*Pmc*2_1, $Eu_5Sn_3S_{12}$: a = 3.908(1), b = 20.115(4), c = 11.451(2) Å; $wR2$ = 0.0519 for 3048 F^2 and 122 parameters; $Eu_4LuSn_3S_{12}$: a = 3.920(1), b = 20.132(4), c = 11.459(2) Å; $wR2$ = 0.0737 for 3298 F^2 and 122 parameters). The structures contain one-dimensional chains of edge-sharing $SnS_2S_{4/2}$ octahedra and corner-sharing $SnS_3S_{2/2}$ trigonal bipyramids, running parallel to [100]. Five europium sites are seven- or eightfold coordinated by sulfur atoms. Lutetium atoms in $Eu_4LuSn_3S_{12}$ show a strong site preference for one of the two Eu^{3+} positions of $Eu_5Sn_3S_{12}$ and no structural disorder was observed. Both compounds show static mixed valence according to $Eu_3^{2+}Eu_2^{3+}Sn_3^{4+}S_{12}^{2-}$ and $Eu_3^{2+}Eu^{3+}Lu^{3+}Sn_3^{4+}S_{12}^{2-}$, which was confirmed by temperature dependent magnetic susceptibility measurements. The experimental magnetic moments of 14.6(1) ($Eu_5Sn_3S_{12}$) and 14.1(1) ($Eu_4LuSn_3S_{12}$) μ_B/f.u. indicate that each of the two sulfides contains three divalent europium atoms per formula unit. Magnetic ordering for $Eu_5Sn_3S_{12}$ and $Eu_4LuSn_3S_{12}$ sets in below 5 and 3 K, respectively. Both sulfides show metamagnetic or spin-flip transitions in the magnetization curves at 3 K (2 K) with full saturation of the europium magnetic moments at 3 K (2 K) and 80 kOe. ^{151}Eu Mössbauer spectra fully confirm the Eu^{2+} and Eu^{3+} site occupancies. At 4.2 K an increase in line width indicates small hyperfine fields at the europium nuclei.

Key words: Europium Compounds, Mixed Valence, Magnetism, Mössbauer Spectroscopy

Introduction

Six ternary europium thiostannates have been described in the literature. Their crystal structures are mostly characterized by arrangements of isolated or connected tetrahedral SnS_4 anions, separated and charge-balanced by europium cations. Compounds with truly divalent europium are $Eu_3Sn_2S_7$ [1], Eu_2SnS_4 [2] and also Eu_2SnS_5, which was erroneously assumed to be isotypic to Sm_2SnS_5 with Eu^{3+} [3]. Magnetic measurements of Eu_2SnS_5 indicated the presence of Eu^{2+} [4], which has been confirmed later by the correct crystal structure which contains S_3^{2-} triangular units [5]. $Eu_4Sn_2S_9$ appears to exhibit dynamic $Eu^{2+/3+}$mixed valence [3], however, this has never been confirmed by ^{151}Eu-Mössbauer spectroscopic or magnetic data. The structural data available for $Eu_4Sn_2S_9$ and our results on $Sr_4Sn_2S_9$ [5, 6] strongly suggest that both compounds are isotypic and that $Eu_4Sn_2S_9$ contains divalent europium exclusively. Recently, the quaternary compounds $Eu_2Sm_2Sn_2S_9$ and $Eu_3Gd_2Sn_2S_9$ have been reported to be isotypic to $Eu_4Sn_2S_9$ [7], but no structural data have been published.

Thus, to date no thiostannate with solely trivalent europium is known. The only compound probably containing static mixed-valence europium on five crystallographically independent Eu sites is $Eu_5Sn_3S_{12}$ [8]. $Eu_5Sn_3S_{12}$ is also the only europium thiostannate with tin in five- and six-fold sulfur coordination, in contrast to the usual SnS_4 tetrahedra. First magnetic measurements [9] supported the formulation $Eu_3^{2+}Eu_2^{3+}Sn_3^{4+}S_{12}^{2-}$, but the existence of static mixed-valence has not yet been confirmed by ^{151}Eu-Mössbauer spectroscopy data. A chemical approach to study this unusual europium thiostannate would be the grad-

Table 1. Crystal data and structure refinement for $Eu_5Sn_3S_{12}$ and $Eu_4LuSn_3S_{12}$.

	$Eu_5Sn_3S_{12}$	$Eu_4LuSn_3S_{12}$
Molar mass, g mol^{-1}	1500.59	1523.60
Crystal system	orthorhombic	orthorhombic
Space group	$Pmc2_1$ (Nr. 26)	$Pmc2_1$ (Nr. 26)
Diffractometer	STOE IPDS	STOE IPDS
Radiation type	Mo K_α (λ = 0.71073 Å)	Mo K_α (λ = 0.71073 Å)
a, Å	3.908(1)	3.920(1)
b, Å	20.115(4)	20.132(4)
c, Å	11.451(2)	11.459(2)
V, Å^3	900.2(3)	904.4(3)
Formula units per cell	$Z = 2$	$Z = 2$
Temperature, K	293(2)	293(2)
Calculated density, g m^{-3}	5.536	5.595
Crystal size, mm^3	$0.07 \times 0.07 \times 0.06$	$0.11 \times 0.05 \times 0.04$
ϕ range; increment, deg	0 – 180; 0.9	0 – 150; 0.9
Irradiation/exposure, min^{-1}	9.5	10.0
Absorption coefficient, mm^{-1}	22.60	24.48
θ range, deg	5.7 – 66.0	5.7 – 66.0
Range in *hkl*	± 5, ± 30 ± 17	± 5, $-30 \rightarrow +27$, $-16 \rightarrow +17$
Total no. reflections	11628	9772
Independent reflections	3748 (R_{int} = 0.065)	3719 (R_{int} = 0.051)
Reflections with $I \geq 2\sigma(I)$	3048	3298
Parameter	122	122
Absorption correction	analytical	analytical
Transmission ratio (min/max)	0.326/0.384	0.161/0.420
Goodness-of-fit (F^2)	0.893	0.981
Final R indices ($I \geq 2\sigma(I)$)	R_1 = 0.0312, wR_2 = 0.0484	R_1 = 0.0321, wR_2 = 0.0720
R Indices (all data)	R_1 = 0.0485, wR_2 = 0.0519	R_1 = 0.0384, wR_2 = 0.0737
Flack parameter	$-0.02(1)$	0.02(1)
Extinction coefficient	0.0004(1)	0.0017(1)
Larg.diff peak/hole, e Å^{-3}	2.09/-1.86	2.23/-3.61

ual substitution of Eu^{2+} by Sr^{2+} or of Eu^{3+} by other trivalent rare earth ions.

In this paper we present single crystal structure determinations of $Eu_5Sn_3S_{12}$ and $Eu_4LuSn_3S_{12}$ with a detailed discussion of the different europium sites and the substitution with lutetium. Magnetic measurements as well as ^{151}Eu/^{119}Sn-Mössbauer spectroscopy were used to determine the valence states at different temperatures.

Experimental Section

Synthesis

Samples of $Eu_5Sn_3S_{12}$ and $Eu_4LuSn_3S_{12}$ were synthesized by heating the elements (Eu, Lu, Sn, purity 99.9 %, Alfa Aesar; S, 99.999 %, ChemPur) or binary sulfides in alumina crucibles, sealed in silica ampoules under a purified argon atmosphere. At first the temperature was raised slowly (50 K h^{-1}) to 1173 K and 1143 K for $Eu_5Sn_3S_{12}$ and $Eu_4LuSn_3S_{12}$, respectively, and kept there for 24 h. After cooling, the samples were homogenized and heated to 1173 K for 24 h. This procedure was repeated once more and resulted in homogeneous dark powders, which were not sensitive to air. Small single crystals suitable for structure determinations were selected from the powder samples.

X-Ray structure determination

X-ray powder patterns of $Eu_5Sn_3S_{12}$ and $Eu_4LuSn_3S_{12}$ samples (STOE Stadi-P, Cu $K_{\alpha 1}$ radiation, Ge monochromator, 7° PSD detector) could be completely indexed by using the crystallographic data from the single crystal experiments. Only traces of unidentified impurity phases were detected.

Small single crystals of $Eu_5Sn_3S_{12}$ and $Eu_4LuSn_3S_{12}$ were selected directly from the samples and inspected by Laue photographs (Mo K_α). Single crystal intensity data were collected at r. t. on a STOE IPDS imaging plate detector (Mo $K_{\alpha 1}$, graphite-monochromator, φ-scan). The IPDS [10] and X-RED [11] software was used for data collection and processing. Analytical absorption corrections were performed using crystal shapes obtained by the FACEIT [12] video system and optimized by the X-SHAPE [13] software.

Refinements of the single crystal data converged rapidly by using the data given in ref. [8] as starting parameters. We used the standard setting of the space group $Pmc2_1$ for $Eu_5Sn_3S_{12}$ and $Eu_4LuSn_3S_{12}$. Refinement cycles with SHELXL-97 [14] converged to final $R1$ values of 0.0312 and 0.0321. Flack parameters of $-0.02(1)$ and 0.02(1) for the

Table 2. Atomic coordinates and equivalent isotropic displacement parameters (U_{eq}, $Å^{-2}$) for $Eu_5Sn_3S_{12}$ and $Eu_4LuSn_3S_{12}$ (space group: $Pmc2_1$).

	Site	*x*	*y*	*z*	U_{eq}
$Eu_5Sn_3S_{12}$:					
Eu1	2*b*	1/2	0.08389(3)	0.8110(1)	0.0092(2)
Eu2	2*b*	1/2	0.10604(3)	0.1749(1)	0.0070(2)
Eu3	2*b*	1/2	0.25938(3)	0.5906(1)	0.0088(2)
Eu4	2*b*	1/2	0.38386(3)	0.2277(1)	0.0093(2)
Eu5	2*b*	1/2	0.58887(3)	0.3534(5)	0.0080(2)
Sn1	2*a*	0	0.08863(4)	0.4837(1)	0.0083(2)
Sn2	2*a*	0	0.25039(4)	0.0000(1)	0.0085(2)
Sn3	2*a*	0	0.57452(4)	0.0131(1)	0.0070(2)
S1	2*b*	1/2	0.0144(2)	0.5511(3)	0.0103(6)
S2	2*b*	1/2	0.1596(2)	0.4004(3)	0.0086(5)
S3	2*b*	1/2	0.2441(2)	0.1515(3)	0.0106(6)
S4	2*b*	1/2	0.5091(2)	0.0706(3)	0.0130(6)
S5	2*b*	1/2	0.7406(2)	0.3562(3)	0.0092(5)
S6	2*a*	0	0.0302(2)	0.2879(3)	0.0080(5)
S7	2*a*	0	0.1256(2)	0.0003(3)	0.0078(5)
S8	2*a*	0	0.1559(2)	0.6634(3)	0.0088(5)
S10	2*a*	0	0.3741(2)	0.0247(3)	0.0075(5)
S11	2*a*	0	0.4866(2)	0.3200(3)	0.0084(5)
S12	2*a*	0	0.6422(2)	0.1969(2)	0.0084(5)
$Eu_4LuSn_3S_{12}$:					
Eu1	2*b*	1/2	0.08356(3)	0.8116(1)	0.0129(2)
Lu	2*b*	1/2	0.10508(3)	0.1736(1)	0.0120(2)
Eu3	2*b*	1/2	0.25860(3)	0.5888(1)	0.0126(2)
Eu4	2*b*	1/2	0.38272(3)	0.2267(1)	0.0135(2)
Eu5	2*b*	1/2	0.58923(3)	0.3516(1)	0.0112(2)
Sn1	2*a*	0	0.08784(5)	0.4814(1)	0.0109(2)
Sn2	2*a*	0	0.24926(4)	0.0000(1)	0.0118(2)
Sn3	2*a*	0	0.57499(4)	0.0126(1)	0.0100(2)
S1	2*b*	1/2	0.0129(2)	0.5485(3)	0.0122(5)
S2	2*b*	1/2	0.1586(2)	0.3973(3)	0.0122(5)
S3	2*b*	1/2	0.2418(2)	0.1513(3)	0.0140(5)
S4	2*b*	1/2	0.5102(2)	0.0727(3)	0.0187(7)
S5	2*b*	1/2	0.7437(2)	0.3557(3)	0.0131(5)
S6	2*a*	0	0.0312(2)	0.2833(3)	0.0109(5)
S7	2*a*	0	0.1240(2)	0.0045(3)	0.0110(5)
S8	2*a*	0	0.1553(2)	0.6615(3)	0.0114(5)
S9	2*a*	0	0.3218(2)	0.4057(3)	0.0142(5)
S10	2*a*	0	0.3733(2)	0.0242(3)	0.0107(5)
S11	2*a*	0	0.4858(2)	0.3194(3)	0.0131(5)
S12	2*a*	0	0.6440(2)	0.1964(3)	0.0121(5)

non-centrosymmetric space group required no refinements with regard to inversion twin domains.

Crystallographic data and experimental details of the data collections are listed in Table 1, final atomic positions and equivalent displacement parameters in Table 2. Selected interatomic distances are given in Table 3. Further details of the structure determinations may be obtained from Fachinformationszentrum Karlsruhe, D-76344 Eggenstein-Leopoldshafen (Germany) by quoting the Registry No's CSD-416862 ($Eu_5Sn_3S_{12}$) and CSD-416861 ($Eu_4LuSn_3S_{12}$).

Physical property measurements

The dc magnetization measurements were carried out using the ACMS option of the QD-PPMS. The samples were enclosed in gelatin capsules and attached to the sample rod assembly. Samples were cooled to the lowest attainable temperature (2 K) in zero field. The susceptibility, $\chi(T)$, was measured while warming the samples in the applied field.

The 21.53 keV transition of ^{151}Eu with an activity of 130 MBq (2 % of the total activity of a $^{151}Sm:EuF_3$ source) and a $Ca^{119m}SnO_3$ source were used for the Mössbauer spectroscopic experiments which were conducted in the usual transmission geometry. The measurements were performed with a commercial helium bath cryostat. The temperature of the absorber was varied between 4.2 K and r. t., while the source was kept at r. t.. The sample was placed in a thin-walled PVC container with at a thickness corresponding to about 10 mg Sn cm^{-2} and Eu cm^{-2}, respectively. For the ^{119m}Sn measurements, a palladium foil of 0.05 mm

Table 3. Interatomic distances (Å) in the structures of $Eu_5Sn_3S_{12}$ and $Eu_4LuSn_3S_{12}$. Standard deviations in units of the last significant digit are given in parentheses.

$Eu_5Sn_3S_{12}$			$Eu_4LuSn_3S_{12}$		
Eu1 —	S8	2.961(2) 2×	Eu1 —	S8	2.981(2) 2×
	S6	3.026(2) 2×		S6	3.046(2) 2×
	S7	3.037(3) 2×		S7	3.064(2) 2×
	S1	3.288(3)		S1	3.334(4)
	S1	3.386(3)		S1	3.338(3)
	∅ Eu–S	3.090		∅ Eu–S	3.107
Eu2 —	S3	2.790(3)	Lu —	S6	2.764(2) 2×
	S6	2.797(2) 2×		S3	2.764(3)
	S2	2.798(3)		S1	2.775(3)
	S1	2.807(3)		S2	2.781(3)
	S7	2.823(2) 2×		S7	2.782(2) 2×
	∅ Eu–S	2.805		∅ Lu–S	2.773
Eu3 —	S2	2.961(3)	Eu3 —	S8	2.977(2) 2×
	S8	2.975(2) 2×		S2	2.978(3)
	S12	3.036(2) 2×		S12	3.034(2) 2×
	S5	3.042(3)		S5	3.058(3)
	S9	3.142(3) 2×		S9	3.141(3) 2×
	∅ Eu–S	3.039		∅ Eu–S	3.043
Eu4 —	S3	2.943(3)	Eu4 —	S3	2.965(3)
	S11	3.034(2) 2×		S10	3.043(2) 2×
	S10	3.043(2) 2×		S11	3.046(2) 2×
	S9	3.089(3) 2×		S9	3.091(3) 2×
	S4	3.095(3)		S4	3.114(3)
	∅ Eu–S	3.046		∅ Eu–S	3.052
Eu5 —	S12	2.860(2) 2×	Eu5 —	S12	2.867(2) 2×
	S11	2.864(2) 2×		S11	2.883(2) 2×
	S10	2.868(2) 2×		S10	2.885(2) 2×
	S5	3.052(3)		S5	3.111(3)
	S4	3.174(4)		S4	3.228(4)
	∅ Eu–S	2.926		∅ Eu–S	2.951
Sn1 —	S8	2.463(3)	Sn1 —	S8	2.471(3)
	S6	2.531(3)		S6	2.541(3)
	S1	2.578(2) 2×		S1	2.590(2) 2×
	S2	2.601(2) 2×		S2	2.607(2) 2×
Sn2 —	S10	2.504(3)	Sn2 —	S10	2.512(3)
	S7	2.510(3)		S7	2.523(3)
	S5	2.561(2) 2×		S5	2.569(2) 2×
	S3	2.616(2) 2×		S3	2.622(2) 2×
Sn3 —	S9	2.393(3)	Sn3 —	S9	2.411(3)
	S4	2.446(2) 2×		S4	2.454(2) 2×
	S12	2.507(3)		S12	2.523(3)
	S11	2.530(3)		S11	2.530(3)

thickness was used to reduce the tin *K* X-rays concurrently emitted by the source. The material for the Mössbauer spectroscopic measurements and the magnetic investigations was taken from the same batch.

Results and Discussion

Crystal chemistry

The crystal structure of $Eu_5Sn_3S_{12}$ is shown in Fig. 1. One-dimensional chains of either edge-sharing $SnS_2S_{4/2}$ octahedra (Sn1, Sn2) or corner-sharing $SnS_3S_{2/2}$ trigonal bipyramids (Sn3) run parallel to [100]. The chains are arranged parallel as a hexagonal rod packing with europium ions filling the trigonal channels. Details of the $^1_\infty[(SnS_2S_{4/2})^{4-}]$ and $^1_\infty[(SnS_3S_{2/2})^{4-}]$ polyanions are shown in Fig. 2. The Sn–S bond lengths are 2.463 – 2.616 Å in the SnS_6 and 2.393 – 2.530 Å in the SnS_5 units. These are slightly longer than in usual SnS_4 tetradedra like in Eu_2SnS_4 (2.40 Å) [2], but remain in the range of the sum of the covalent radii of 2.44 Å [15]. The small elongation is surely a consequence of the higher coordination number, so we can assume tin as Sn^{4+} from the viewpoint of the Sn–S bond lengths.

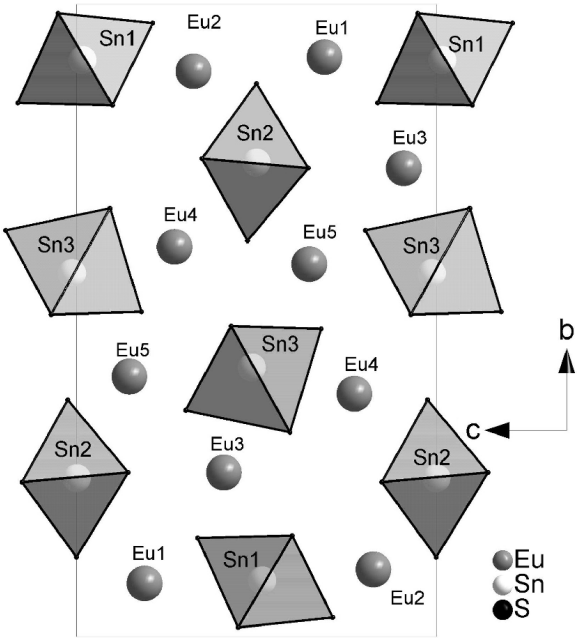

Fig. 1. Crystal structure of $Eu_5Sn_3S_{12}$, projection onto the *bc* plane. The octahedral (Sn1, Sn2) or trigonal-bipyramidal (Sn3) tin coordination is emphasized.

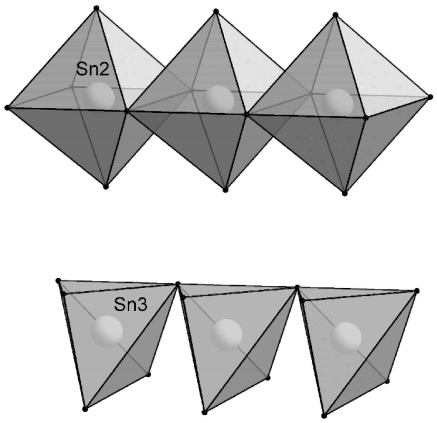

Fig. 2. One-dimensional polyanions in $Eu_5Sn_3S_{12}$. $^1_\infty[(Sn S_2S_{4/2})^{4-}]$ (edge-sharing octahedra) and $^1_\infty[(SnS_3S_{2/2})^{4-}]$ (corner-sharing trigonal bipyramids) chains run along [100].

$Eu_5Sn_3S_{12}$ contains five crystallographically different Eu positions with *m*.. site symmetry. Seven or eight sulfur atoms surround the europium atoms forming trigonal prisms with one or two square faces capped by additional sulfur atoms. Fig. 3 shows the five similar coordination polyhedra. Altogether the Eu–S distances cover a wide range from 2.790 to 3.386 Å. An assignment of the europium valences seems straightforward as already proposed by Jaulmes and Julien-Pouzol [8]. Eu1, Eu3 and Eu4 have eight neighbors with average Eu–S bond lengths of 3.090, 3.039 and 3.046 Å, respectively, and no distance shorter than 2.961 Å. In contrast, Eu2 has only seven neighbors, the mean Eu–S distance is 2.805 Å and no bond is longer than 2.823 Å. Eu5 seems to be somewhat intermediate, a phenomenon not noticed by Jaulmes and Julien-Pouzol [8]. Eight sulfur atoms surround Eu5 with Eu–S distances up to 3.174, similar to Eu3 or Eu4. But the six sulfur atoms forming the trigonal prism are only 2.864 or 2.860 Å away, as depicted in Fig. 3. This results in an average distance of 2.926 Å, which is halfway between that of the Eu1, Eu3, Eu4 ($\sim$ 3.05 Å) and the Eu2 sites (2.805 Å). From this bond length consideration we can reliably assign the sites Eu1, Eu3 and Eu4 to divalent europium, and Eu2 to trivalent. The Eu5 position is not that clear, however, trivalent europium on this site seems more probable due to the short nearest neighbor distances and also because of a charge balanced formula according to $Eu_3^{2+}Eu_2^{3+}Sn_3^{4+}S_{12}^{2-}$.

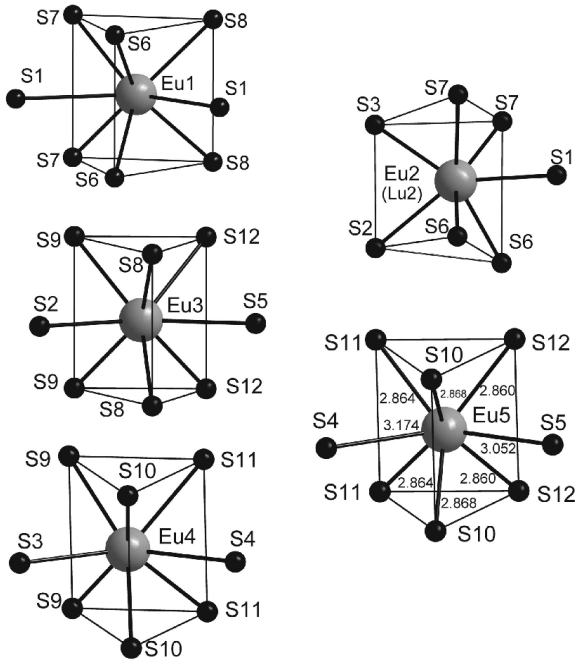

Fig. 3. Coordination polyhedra of the Eu atoms in $Eu_5Sn_3S_{12}$ and $Eu_4LuSn_3S_{12}$.

In a next step we tried to substitute the Eu^{3+} sites by another trivalent rare earth ion. We chose lutetium due to the similar ionic radii of Lu^{3+} and Eu^{3+} and also because of the nonmagnetic f^{14} shell of Lu^{3+}.

Furthermore it is possible to distinguish europium and lutetium in the single crystal X-ray experiment. All attempts to occupy both Eu^{3+} sites in $Eu_5Sn_3S_{12}$ with Lu^{3+} failed, and thus we did not succeed in synthesizing $Eu_3Lu_2Sn_3S_{12}$. In contrast, we were able to prepare phase pure $Eu_4LuSn_3S_{12}$. The single crystal structure determination confirmed the $Eu_5Sn_3S_{12}$ structure for $Eu_4LuSn_3S_{12}$ (see Tables 1 and 2) with very similar structural parameters. The Lu–S distances are slightly shorter than the corresponding Eu5–S distances and range from 2.764 to 2.782 Å, whereas all Sn–S bonds remain almost unchanged. Exclusively the Eu2 (Eu^{3+}) site of the $Eu_5Sn_3S_{12}$-type is substituted by Lu leading to the ionic formulation $Eu_3^{2+}Eu^{3+}Lu^{3+}Sn_3^{4+}S_{12}^{2-}$. No indication of Eu/Lu disorder was detected. Interestingly, Eu2 is exactly the position which we could undoubtedly assign to Eu^{3+}. In contrast to this, the "intermediate" Eu^{3+} site (Eu5) in $Eu_5Sn_3S_{12}$ is not occupied by Lu^{3+} at all. The reason why this position apparently gives no fit for lutetium or other trivalent rare earth ions is not clear. Further substitution experiments are therefore in progress in order to study the interesting site preferences of trivalent rare earth or divalent strontium ions in $Eu_5Sn_3S_{12}$.

Magnetic properties

Fig. 4 shows the dc susceptibility (χ) and inverse susceptibility (χ^{-1}) of $Eu_5Sn_3S_{12}$ measured under a field of 5 kOe. The susceptibility increases with decreasing temperature in the entire temperature range without any signs of magnetic ordering at the lowest temperatures. There is a small anomaly at 65 – 85 K, which coincides with the ferromagnetic ordering of EuO indicating a trace amount of impurity. We could not detect any other impurity affecting the magnetic properties of the parent compound. $\chi(T)$ follows the Curie-Weiss law above 100 K. The paramagnetic Curie temperature (θ_p) derived from the linear region of the χ^{-1} *vs.* T plot at high temperatures is close to zero (0.02 K), with an effective Bohr magneton number of 14.6(1) μ_B/f.u. According to an ionic formula splitting $Eu_3^{2+}Eu_2^{3+}Sn_3^{4+}S_{12}^{2-}$, three of the five europium atoms carry a nonzero magnetic moment. Thus, the experimentally observed moment is close to the theoretical value of $\sqrt{3} \times 7.94 = 13.75\ \mu_B$/f.u. [16].

The low field susceptibility, measured at 100 Oe in zero field (ZFC) and field cooled (FC) states of the sample, is shown as an insert in Fig. 4. There

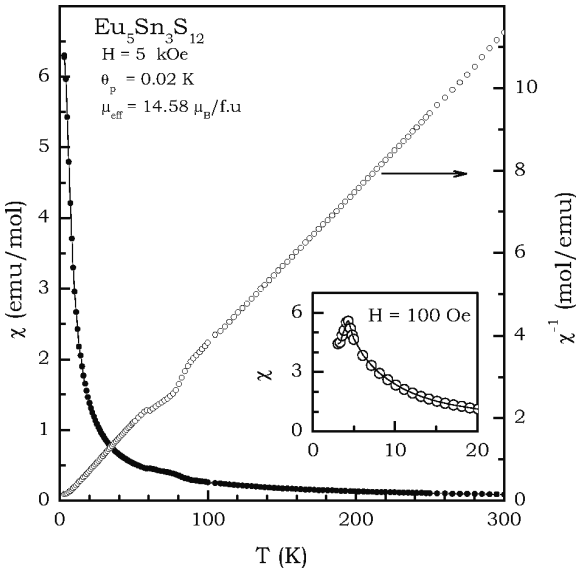

Fig. 4. dc susceptibility (χ) and inverse susceptibility (χ^{-1}) for $Eu_5Sn_3S_{12}$ measured at H = 5 kOe. The insert shows the susceptibility measured at H = 100 Oe for ZFC and FC states of the sample.

is no bifurcation of the ZFC–FC curves, but a peak around 4 K is clearly seen in both states, indicating antiferromagnetic ordering. The susceptibility measurements already establish a field induced change in the magnetic structure at temperatures below 5 K. In order to probe this behavior in detail, we measured the isothermal magnetization M(H) at several temperatures. In Fig. 5, we have plotted M(H) for $Eu_5Sn_3S_{12}$ measured at T = 3, 10, 30, 100 and 300 K and up to 80 kOe. There is a clear change in the magnetism of this compound, as one moves from high to low temperatures. M(H) measured at 3 K exhibits a metamagnetic or spin-flip transition around 10 kOe and saturates at fields above 30 kOe. The saturation moment at 80 kOe, assuming three Eu^{2+}, is about 7 μ_B, close to the expected value for Eu^{2+}. It should also be noted that at low fields ($<$ 10 kOe) M(H), there is a small loop in the increasing and decreasing cycles of the ramping field. There is a drastic change in the magnetism of this compound as one moves from 3 to 10 K. The M(H) at 10 K increases with field, but does not exhibit any step or hysteresis. The curve is continuously changing without any signs of saturation up to 80 kOe. M(H) at 30 K is similar to the 10 K pattern in terms of the curvature. The curve is not linear up to high fields, as if the magnetic interactions were persistent up to such a high temperature, even though antiferromagnetic ordering

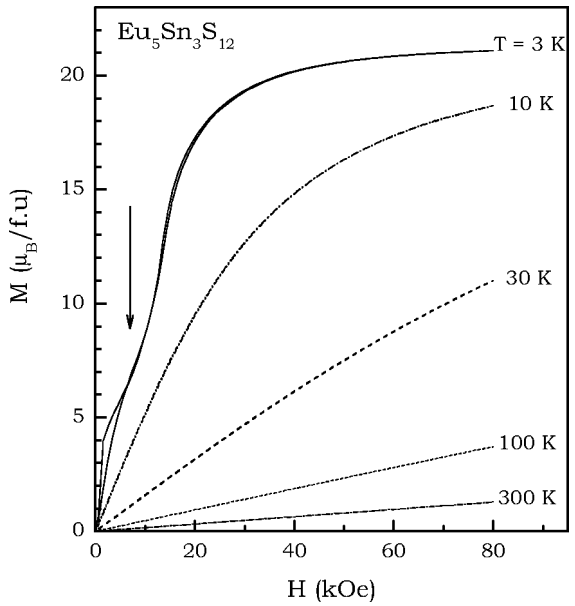

Fig. 5. Magnetization as a function of ramping field measured at various temperatures for $Eu_5Sn_3S_{12}$. The vertical arrow in the plot at 3 K indicates the metamagnetic or spin-flip transition.

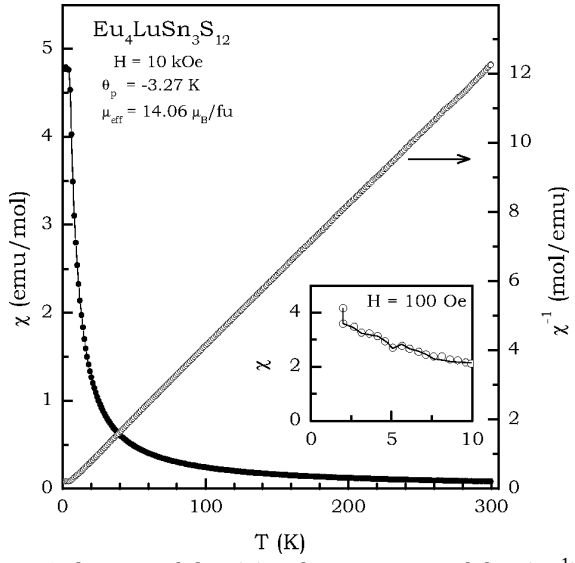

Fig. 6. dc susceptibility (χ) and inverse susceptibility (χ^{-1}) for $Eu_4LuSn_3S_{12}$ measured at H = 10 kOe. The insert shows the susceptibility measured at H = 100 Oe for ZFC and FC states of the sample.

(from low field susceptibility) was observed at 4 K. The high temperature M(H) curves measured at T = 100 and 300 K are linear with field as expected for the paramagnetic state.

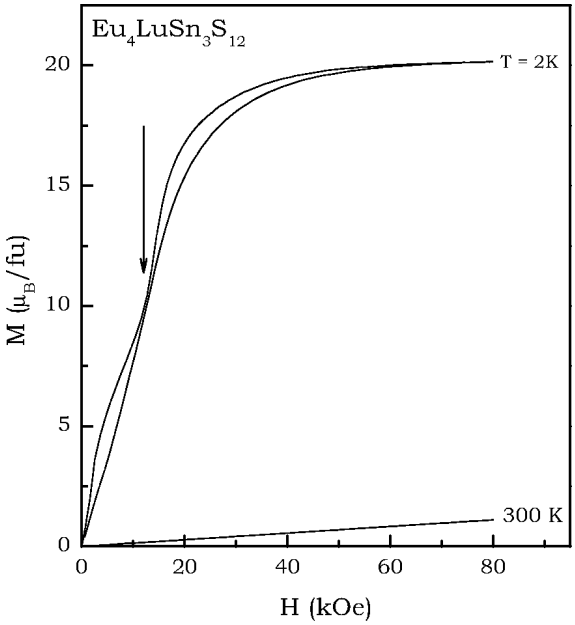

Fig. 7. Magnetization as a function of ramping field measured at lowest (2 K) and r. t. (300 K) for $Eu_4LuSn_3S_{12}$. The vertical arrow in the plot at 2 K indicates the metamagnetic or spin-flip transition.

In Fig. 6, we show the dc susceptibility for $Eu_4LuSn_3S_{12}$ measured in a field of 10 kOe. As can be seen from the plot of $\chi(T)$, there is no clear magnetic ordering (peak in χ) down to 2 K, however, the flat region below 4 K in the inverse susceptibility (χ^{-1}) indicates subtle changes in the magnetism. From the Curie-Weiss fitting in the linear region of χ^{-1} at high temperatures ($>$ 100 K), the values of θ_p and μ_{eff} are -3.2 K and 14.1(1) μ_B/f.u. respectively, similar to $Eu_5Sn_3S_{12}$. The value of μ_{eff} reveals that Lu^{3+} replaces one Eu^{3+}, leaving the Eu^{2+} ions undisturbed. In the insert of Fig. 6, we have also plotted the low field susceptibility of $Eu_4LuSn_3S_{12}$ measured in the ZFC–FC states. $\chi(T)$ measured under a 100 Oe field shows no bifurcation in the ZFC–FC curves. The isothermal magnetization of $Eu_4LuSn_3S_{12}$ measured at 2 K is plotted in Fig. 7. Similar to the parent compound, $Eu_4LuSn_3S_{12}$ also exhibits a metamagnetic or spin-flip transition around 10 kOe, and saturates at higher fields. The saturation moment is also of the same value, ~ 7 μ_B/Eu. The M(H) loop is hysteretic between 0 and 10 kOe and again between 10 and 50 kOe. The M(H) curve at 2 K and low field susceptibility indicates a subtle change in magnetism of this compound below 4 K, which is

Table 4. Fitting parameters of ^{151}Eu Mössbauer measurements of $Eu_5Sn_3S_{12}$ and $Eu_4LuSn_3S_{12}$. Numbers in parentheses represent the statistical errors in the last digit. δ = isomer shift, Γ = experimental line width.

Compound	T (K)	δ_1 (mm s^{-1})	Γ_1 (mm s^{-1})	δ_2 (mm s^{-1})	Γ_2 (mm s^{-1})	χ^2	Eu^{2+}/Eu^{3+}
$Eu_5Sn_3S_{12}$	298	−12.12(1)	3.06(4)	0.41(1)	3.08(5)	1.52	54(2)/46(2)
	78	−12.15(9)	3.05(3)	0.58(1)	2.82(3)	1.70	57(2)/43(2)
	4.2	−11.95(2)	4.46(2)	0.53(6)	2.72(2)	1.09	60(2)/40(2)
$Eu_4LuSn_3S_{12}$	298	−12.15(8)	3.07(3)	0.33(2)	3.37(5)	1.33	63(3)/36(3)
	78	−12.09(4)	3.22(2)	0.50(7)	2.81(2)	1.92	66(3)/34(3)
	4.2	−12.06(2)	4.58(2)	0.51(4)	2.70(1)	1.09	69(3)/31(3)

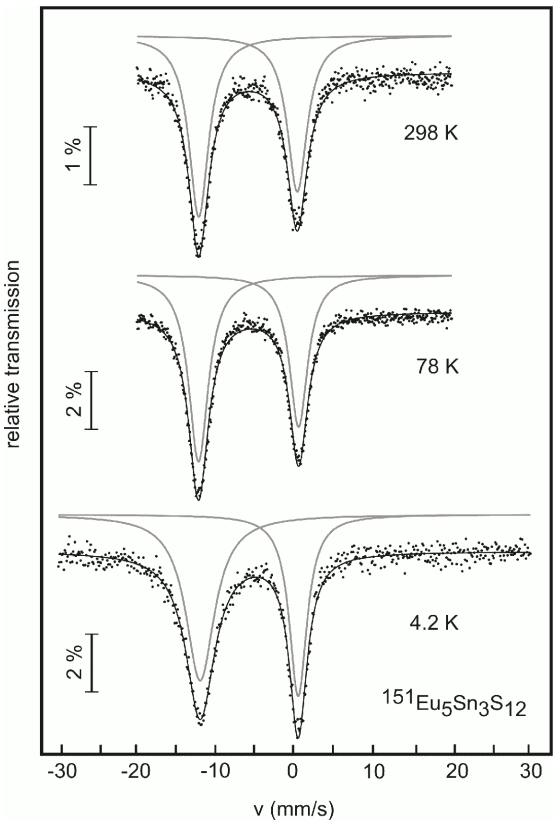

Fig. 8. Experimental and simulated ^{151}Eu Mössbauer spectra of $Eu_5Sn_3S_{12}$ at various temperatures.

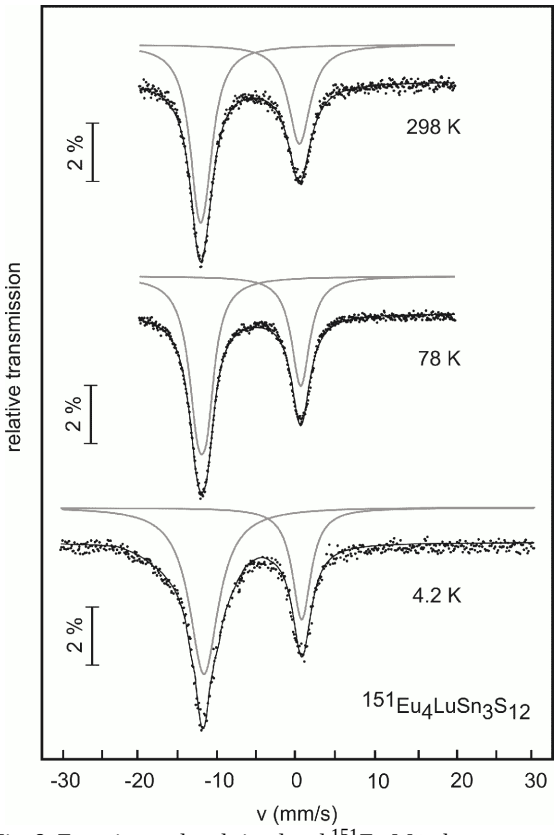

Fig. 9. Experimental and simulated ^{151}Eu Mössbauer spectra of $Eu_4LuSn_3S_{12}$ at various temperatures.

essentially dependent on the ordering of the Eu^{2+} moments.

^{151}Eu and ^{119}Sn Mössbauer spectroscopy

The ^{151}Eu Mössbauer spectra of $Eu_5Sn_3S_{12}$ at 298, 78, and 4.2 K are presented in Fig. 8 together with transmission integral fits. The corresponding fitting parameters are listed in Table 4. Over the whole temperature range we observe two signals at isomer shifts around −12 and 0.5 mm/s, indicating a static mixed valence of Eu^{2+} and Eu^{3+}. There is no pronounced change in the isomer shifts with decreasing temperature. At 4.2 K the area ratio of the two signals Eu^{2+}/Eu^{3+} is 60/40, in good agreement with the ionic formula $Eu_3^{2+}Eu_2^{3+}Sn_3^{4+}S_{12}^{2-}$ as discussed above. The Eu^{2+} signal shows a slightly enhanced line width at 4.2 K, indicative of a very small hyperfine field and the onset of magnetic ordering, in agreement with the magnetic data.

The ^{151}Eu spectra of the quaternary sulfide $Eu_4LuSn_3S_{12}$ are similar to those of $Eu_5Sn_3S_{12}$

Table 5. Fitting parameters of ^{119}Sn Mössbauer measurements of $Eu_5Sn_3S_{12}$ and $Eu_4LuSn_3S_{12}$. Numbers in parentheses represent the statistical errors in the last digit. δ = isomer shift, Γ = experimental line width, ΔE_Q = electric quadrupole splitting parameter. The second signal observed in the low temperature measurements of $Eu_4LuSn_3S_{12}$ has an area of *ca.* 3 %.

Compound	T (K)	δ_1 (mm s^{-1})	ΔE_{Q1} (mm s^{-1})	Γ_1 (mm s^{-1})	δ_2 (mm s^{-1})	ΔE_{Q2} (mm s^{-1})	Γ_2 (mm s^{-1})	χ^2
$Eu_5Sn_3S_{12}$	298	1.11(4)	0.56(1)	0.88(2)	–	–	–	0.93
	78	1.14(8)	0.58(1)	0.89(2)	–	–	–	0.95
	4.2	1.14(3)	0.67(6)	1.11(1)	–	–	–	0.98
$Eu_4LuSn_3S_{12}$	298	1.15(4)	0.56(1)	0.90(1)	–	–	–	0.98
	78	1.12(2)	0.57(4)	0.92(8)	3.64(5)	0.80(8)	1.17(2)	1.09
	4.2	1.10(1)	0.55(1)	1.03(2)	3.33(3)	0.59(7)	1.26(4)	1.64

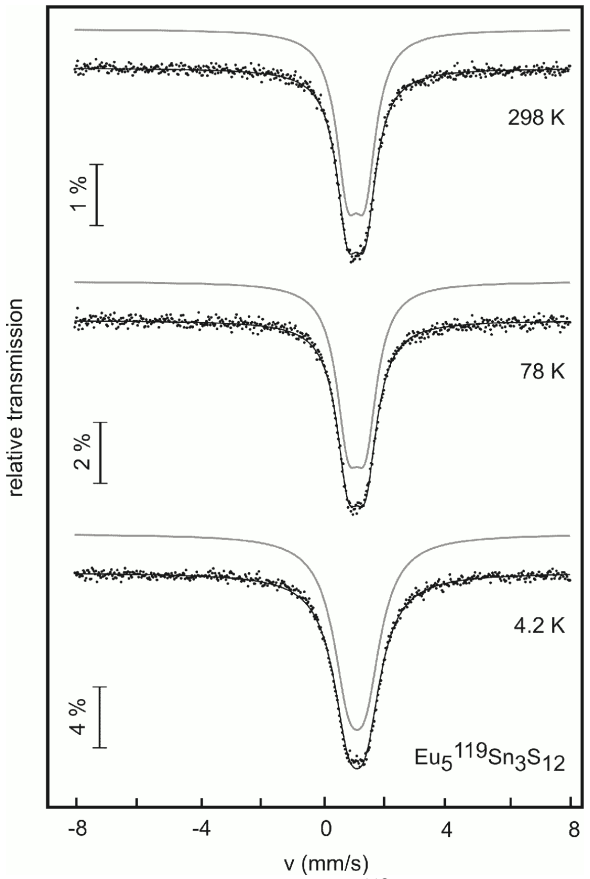

Fig. 10. Experimental and simulated ^{119}Sn Mössbauer spectra of $Eu_5Sn_3S_{12}$ at various temperatures.

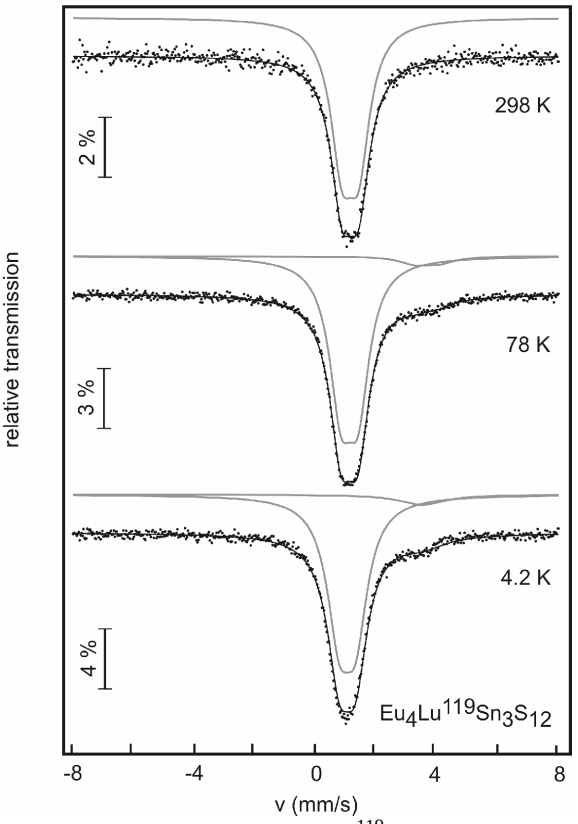

Fig. 11. Experimental and simulated ^{119}Sn Mössbauer spectra of $Eu_4LuSn_3S_{12}$ at various temperatures.

(Fig. 9). Because one of the trivalent europium sites is now occupied by lutetium, the portion of divalent europium is higher in this compound. The Eu^{2+}/Eu^{3+} ratio of 69(3)/31(3) at 4.2 K is close to the expected ratio of 75/25. The isomer shifts of the quaternary sample are close to the values found for $Eu_5Sn_3S_{12}$. For $Eu_4LuSn_3S_{12}$ the line width also increases at 4.2 K due to the onset of magnetic ordering. For both compounds the magnetic hyperfine fields at 4.2 K are small and can not be resolved. Therefore the spectra were fitted with the increased line widths.

The ^{119}Sn spectra of $Eu_5Sn_3S_{12}$ and $Eu_4LuSn_3S_{12}$ at 298, 78, and 4.2 K are presented in Figs. 10 and 11 and the corresponding parameters in Table 5. The isomer shifts are similar for both compounds over the whole temperature range. They compare well with the isomer shift of 1.3 mm/s for SnS_2 and 1.15 mm/s for the tetravalent tin site in Sn_2S_3 [17]. Due to the

non-cubic site symmetry, the tin spectra are subject to weak quadrupole splitting. At 4.2 K the line width of both sulfides slightly increases, most likely due to very small transferred magnetic hyperfine fields. At 78 and 4.2 K, the ^{119}Sn Mössbauer spectra of $Eu_4LuSn_3S_{12}$ revealed a small additional signal around δ = 3.5 mm/s, most likely due to a trace amount of a SnS impurity (δ = 3.4 mm/s [2]).

Acknowledgements

This work was supported by the Deutsche Forschungsgemeinschaft. S. R. and C. P. S. are indebted to the Alexander von Humboldt-Stiftung and the NRW Graduate School of Chemistry for research grants.

[1] S. Jaulmes, M. Julien-Pouzol, *Acta Crystallogr.* **1977**, *B33*, 3898 – 3899.
[2] R. Pocha, M. Tampier, R. D. Hofmann, B. D. Mosel, R. Pöttgen, D. Johrendt, *Z. Anorg. Allg. Chem.* **2003**, *629*, 1379 – 1384.
[3] J. Flahaut, P. Laruelle, M. Guittard, S. Jaulmes, M. Julien-Pouzol, C. Lavenant, *J. Solid State Chem.* **1979**, *29*, 125 – 136.
[4] M. Guittard, S. Jaulmes, M. Julien-Pouzol, E. Barthelemy, J. Flahaut, *C. R. Acad. Sci., Ser. 2*, **1983**, *296*, 249 – 251.
[5] R. Pocha, Ph. D. Thesis, Universität München, **2004**.
[6] R. Pocha, D. Johrendt, *Inorg. Chem.* **2004**, *43*, 6830 – 6837.
[7] V. A. Gasymov, O. M. Aliev, V. M. Ragimova, E. A. Bakhshalieva, *Kimya Problemlari Jurnali* **2005**, 128 – 130.
[8] S. Jaulmes, M. Julien-Pouzol, *Acta Crystallogr.* **1977**, *B33*, 1191 – 1193.
[9] T. I. Volkonskaya, A. G. Gorobets, S. A. Kizhaev, I. A. Smirnov, V. V. Tikhonov, M. Guittard, C. Lavenant, J. Flahaut, *Phys. Status Solidi A* **1980**, *57*, 731 – 734.
[10] IPDS-Software, Rev. 2.93. Stoe & Cie GmbH, Darmstadt (Germany) **2000**.
[11] X-RED32, X-RED data reduction Rev. 1.26. Stoe & Cie GmbH, Darmstadt (Germany) **2004**.
[12] FACEIT, Video System. Stoe & Cie GmbH, Darmstadt (Germany) **1998**.
[13] X-SHAPE, Crystal Optimization for Numerical Absorption Correction. Stoe & Cie GmbH, Darmstadt (Germany) **1999**.
[14] G. M. Sheldrick SHELXL, Program for crystal structure refinement., Universität Göttingen, Göttingen (Germany) **1997**.
[15] L. Pauling; *Die Natur der chemischen Bindung*, Verlag Chemie GmbH, Weinheim (Germany) **1976**.
[16] H. Lueken; *Magnetochemie*, Teubner, Stuttgart (Germany) **1999**.
[17] P. E. Lippens, *Phys. Rev. B* **1999**, *60*, 4576 – 4586.